

See discussions, stats, and author profiles for this publication at: <https://www.researchgate.net/publication/373044160>

Signal-to-Interference Ratio Coverage-Aware Multi-Access Edge Computing in Intelligent Reflecting Surfaces-Assisted Multi-Tier 6G Networks

Article in SN Computer Science · August 2023

DOI: 10.1007/s42979-023-02044-0

CITATIONS

0

READS

18

2 authors:



Mobasshir Mahbub
Ahsanullah University of Science & Tech

53 PUBLICATIONS 281 CITATIONS

[SEE PROFILE](#)



Raed Shubair
New York University Abu Dhabi

477 PUBLICATIONS 6,775 CITATIONS

[SEE PROFILE](#)

Some of the authors of this publication are also working on these related projects:



NB-IoT [View project](#)



IIoT Wireless Communications [View project](#)



Signal-to-Interference Ratio Coverage-Aware Multi-Access Edge Computing in Intelligent Reflecting Surfaces-Assisted Multi-Tier 6G Networks

Mobasshir Mahbub¹ · Raed M. Shubair¹

Received: 20 February 2023 / Accepted: 6 June 2023
© The Author(s), under exclusive licence to Springer Nature Singapore Pte Ltd 2023

Abstract

Beyond fifth-generation (5G) or sixth-generation (6G) communication systems will feature a significant number of gadgets and a wide range of services, most of which will have steep processing needs and stringent latency constraints. To meet such expectations, multi-access edge computing (MEC) will play a crucial function in the evolution of cloud systems. Users may offload their tasks/programs to edge servers, which are capable of executing computational operations and reacting rapidly with an output. Intelligent reflecting surface (IRS) is already recognized as one of the major facilitating mechanisms for forthcoming wireless transmission networks because of its capability to dynamically adjust the phase shift of reflecting electromagnetic signals to establish a suitable propagation atmosphere. Since IRS can enhance the propagation environment both academia and industry are already engaged in research on the inclusion of IRS technology in MEC to improve the latency requirement. Therefore, the work aimed to enhance the uplink signal-to-interference ratio (SIR)-coverage probability-aware or SIR-threshold-based coverage probability-aware communication and computation capacity of a latency-aware MEC system attached to a micro base station of a two-tier network by optimal resource allocation, i.e., transmit power and bandwidth. The work deployed IRS in a micro cell operating under a macro cell base station, i.e., forming a two-tier network aiming to complete computation tasks within the required latency assuring energy and bandwidth efficiency. It compared the deployment of a MEC system considering both the conventional two-tier network and the IRS-assisted two-tier network in which the IRS is deployed between the micro base station and the user. The work adopting MATLAB software-based simulation approach derived that the deployment of an IRS can offer successful task completion within the required task completion time with significantly minimizing the energy and bandwidth consumption.

Keywords 6G · IRS · MEC · SIR · Coverage probability

Introduction

While fifth-generation (5G) cellular communication infrastructures are being implemented globally [1–3], a slew of unique applications and uses inspired by modern trends are

actively being developed, putting 5G's capabilities to the test [4]. This has prompted experts to reconsider and move toward the forthcoming generation of mobile communication systems, designated "6G." 6G cellular communication networks [5–7] are predicted to usher in a disruptive paradigm shift in wireless networking by achieving extraordinary network capabilities to meet the needs of the emerging data-driven society.

To accomplish all of the aspirations that 5G cannot fulfill, 6G networks are intended to be more competent, intelligent, consistent, extensible, and power-efficient [8]. The advancement of 6G is expected to center on a slew of new needs, including massive low-latency machine-type communications (mLLMTC), Further extended mobile broadband (FeMBB), mobile broadband and low-latency (MBBLL), and ultra-massive Machine-Type Communications

This article is part of the topical collection "Research Trends in Communication and Network Technologies" guest edited by Anshul Verma, Pradeepika Verma and Kiran Kumar Pattanaik.

✉ Mobasshir Mahbub
mobasshir@ieee.org

Raed M. Shubair
raed.shubair@ieee.org; raed.shubair@nyu.edu

¹ Department of Electrical and Computer Engineering, New York University (NYU) Abu Dhabi, Abu Dhabi, UAE

(umMTC) [9, 10]. Many novel concepts in communication systems have emerged recently, including communication beyond sub-6GHz to THz [11], edge intelligence (EI) [12], non-orthogonal multiple access (NOMA) [13], intelligent reflecting surfaces/reconfigurable intelligent surfaces (IRS/RIS) [14–16], self-sustaining networks (SSN) [17], and swarm networks [18], etc. These ideas are maturing into full-fledged technologies capable of powering subsequent generations of communications systems. Unmanned aerial vehicles (UAV), holographic telepresence (HT), extended reality (XR), Industry 5.0, smart grid 2.0, etc. on the contrary, are anticipated to appear as mainstream uses of forthcoming communication networks [19].

6G mobile telephony networks, as currently envisioned, are predicted to produce exceptional peak data rates of more than 1 Tbps. The end-to-end latency is expected to be lower than 1 ms [19]. The network's accessibility and dependability are predicted to exceed 99.99999%. To enable the internet of everything (IoE), an extraordinarily high connectivity density of above 10^7 devices/km² is projected to be enabled. The spectrum capacity of 6G will be more than five times that of 5G, with support for user maneuverability up to 1000 km/h envisaged [19–21].

With the exponential progress of transmission systems in recent times, a diversity of computation-intensive and latency-sensitive application scenarios, such as virtual reality, augmented reality, autonomous driving, and unmanned aerial vehicles, are appeared to deliver real-time machine-to-machine and machine-to-human communications [21]. The effectiveness of these modern innovations is dependent on the next version of wireless networks being able to accommodate enormous devices for real-time processing, connectivity, and control. End-user gadgets are typically endowed with capacity-limited batteries and a low-performance central processing unit (CPU) because of production cost considerations and severe device space constraints [18]. Thus, how to improve device computational capabilities to manage intense computation loads with severe latency constraints becomes a major concern in future networks [22]. Traditionally, cloud computing technology is required to be used to provide devices with plentiful computational resources. However, since the cloud servers are often located in the distant network core, they may have a considerable computational delay.

To address the aforesaid issue, a new computing paradigm named MEC has arisen [23–25] attracting considerable interest from both industries and academia. MEC is envisaged as a prospective paradigm that makes the use of edge nodes that are positioned near end-user devices. Edge nodes in mobile networks, such as base stations can be endowed with powerful computation and storage capabilities. MEC allows users to delegate computational tasks/workloads to edge nodes for processing [26]. Since enormous local

equipment may be required to offload work to edge servers for computation, effective offloading is critical in MEC [27].

In the ultra-dense multi-tier network [28] typically formed by small cells, i.e., micro, pico, femto cell, and macro cell base stations in which a lot of small/tiny base stations can be implemented to decrease the separation distance between base stations and user equipment/user devices (UEs) or ensure direct or line-of-sight (LoS) between them to offer improved offloading links [29, 30].

Computation offloading is divided into two models [31]: binary offloading and partial offloading. Partially offloading, in particular, permits a computation (task) to be divided into two pieces. One half is executed locally, while the other is sent to the server for processing. Binary offloading, in contrast, necessitates that a task is processed either locally or at the edge server. Minimizing execution latency and minimizing energy usage are two valid goals for computational task offloading [32] in MEC technologies.

Recent breakthroughs in programmable meta-materials make it easier to create intelligent reflecting surfaces to improve the spectrum and energy efficiency of wireless transmission systems [33]. IRS has lately surfaced as a possible method for addressing bandwidth and energy challenges. IRS is made up of several low-cost passively reflecting components with customizable phase shifts [34–36]. The radiated signals from several pathways can be merged coherently to increase the transmission rate at the MEC server by correctly modifying the phase shift of the reflecting components (of IRS). IRS achieves gain by the summation of reflection-aided beamforming gain and virtual array gain. To explain, virtual array gain or virtual gain is generated by integrating both IRS-reflected and direct signals, whereas reflection-aided beamforming gain is acquired by actively regulating the phase shift caused by the IRS components. By integrating these two categories of benefits, the IRS achieves the ability to increase the offloading rate of success of the equipment, hence enhancing the viability of MEC technologies [37].

Motivations The motivations to perform this research is enlisted below -

- End devices or user devices usually have very limited computation capacity. Therefore, to complete a computation (of a task) they require offloading the task to a cloud server or an edge computing server [23].
- Nowadays, latency-sensitive applications like video analytics, video surveillance, augmented/virtual reality (AR/VR), etc. require faster task processing to derive a faster output/result. Moreover, sophisticated internet of things (IoT) applications such as sensor data analytics for eHealthcare, smart farming, smart surveillance, industrial IoT, facial or fingerprint recognition, etc. require very high computation or task processing to derive an

output within the latency requirement. Multi-access edge computing becomes a prominent solution for such applications to complete a task processing within the latency requirement [26].

- On the other hand, the deployment of the IRS improves the network performance assuring energy efficiency [35]. Moreover, the implementation of IRS is capable of reducing the end-to-end latency by enhancing the transmission rate [34].
- Typically end devices have low battery capacity and in the case of IRS-assisted network end devices can offload computation tasks with a lower transmit power (due to the improved transmission link capacity). Therefore, the deployment of IRS will preserve the battery of end devices, e.g. smartphones, sensor/IoT devices, etc [36].
- Interference has a significant influence on the performance of a communications network [38]. For forthcoming multi-tier networks, it is a significant matter of concern. Thereby, the minimization of interference to improve or maximize the SIR is a notable research issue nowadays [39]. Measurement and analysis in terms of SIR coverage-aware transmission planning are unavailable in the context of IRS-assisted MEC systems.

The above-mentioned terms encouraged this work to perform the targeted research.

Contribution of this work Briefly to be said, the work aimed to perform efficient computation offloading to the MEC server assuring optimal resource allocation. The contributions of this research are enlisted below:

- The work formulated a MEC network model considering a two-tier network formed by macro and micro cell base station tiers in which a MEC server is attached to the micro base station to provide edge computing facilities to edge users or end users.
- The work aimed to allocate optimal or energy efficient transmit power and latency-aware optimal bandwidth in terms of SIR-threshold-aware coverage probability for user devices especially cell-edge devices. Because if the cell-edge users can obtain favorable coverage then the users at mid of the cell or near the base station will surely get better coverage. The SIR-threshold-aware coverage probability-based network resource allocation, i.e., power and bandwidth allocation for the MEC network can be mentioned as a novel contribution of this work because according to the best of the authors' knowledge no prior work considers SIR-threshold-aware coverage probability-based analysis and measurement.
- The research targeted efficient computational task offloading and processing in terms of task completion time (overall latency for a task) requirement and battery-level or power constrained at the user device.

- To efficiently allocate network resources and to offload computational tasks the work developed two algorithms.
- The development of SIR-threshold-based coverage probability-aware algorithms can be regarded as another novel contribution of this work.
- To maximize the energy and bandwidth efficiency the research deployed IRS (in a micro cell) and compared it with the conventional network.

Typically multi-tier networks are formed by macro cell tier, micro cell tier, pico cell tier, and femto cell tier. Compared to the pico (very short-range coverage) and femto (indoor) cell tier, micro cell tier base stations generally have a larger coverage extent. Therefore, there is a significant probability of non-line of sight (NLoS) channels, especially in the urban scenario and due to the impact of the interference from the macro cell in the context of forthcoming cellular networks, i.e., 6G networks the desired coverage, namely, data rate, latency may not be obtained. Since the pico cells offer coverage over a short range and the femto cell is usually for indoor communication, the NLoS problem is not much significant in these types of cells, therefore, the work considered a two-tier network in which a micro cell operates under a macro cell base station. As pico cells offer coverage over a short range and femto cells are indoor they have less impact on a network in terms of interference and to keep the analysis simpler the work considered only the impact of the interference of a macro cell tier/base station and interfering micro base stations on the serving micro base station. This is the reason behind selecting a two-tier network.

Related Literature

The work in this section included a review of prior literature and works to provide insight into prior and ongoing work on the relative research topic.

Chen et al. [40] investigated an IRS-assisted wireless powered-MEC system, where both NOMA and time division multiple access (TDMA) techniques are considered for task offloading. The work proposed three different types of dynamic IRS beamforming schemes for adjusting the beamforming vector of IRS. Problems for maximizing the computation rate are formulated for the NOMA and TDMA schemes, respectively, by the joint optimization of the IRS beamforming and resource allocation.

Wang et al. [41] studied an IRS-assisted MEC system with a NOMA scheme. The energy efficiency is optimized by the joint optimization of the local computing frequency, task offloading power, phase-shift matrix of IRS, and receiving beamforming.

Zhou et al. [42] considered an IRS-aided MEC system, where an IRS is implemented to support computational task

offloading from two user equipment to an edge cloud. The research formulated an optimization problem to reduce the sum delay of the users by controlling the passive reflection of IRS and users' task-offloading scheduling considering the discrete-phase constraint of IRS.

Wang et al. [43] proposed an IRS/UAV-based MEC scheme for traffic-offloading in a 6G network utilizing radio-frequency (RF) power. In this network, a UAV is acting as a MEC server to receive data from users. The work formulated a problem to minimize task processing time jointly optimizing UAV trajectory and flying time, phase shifts of IRS elements, resource allocation, and user scheduling.

Park et al. [44] considered a MEC system supported by a UAV-based communication network incorporating IRS in the case of 6G THz networks. The work jointly optimized the computation power, the phase shift of IRS, and allocation of THz sub-band to reduce network latency.

Bai et al. [45] proposed to employ IRS in a wireless powered-MEC system that offers communication links for both wireless energy transfer (WET) and computation offloading. The proposed system is based on orthogonal frequency-division multiplexing (OFDM) scheme. The work developed a framework to minimize the overall energy consumption of the network.

Tan et al. [46] considered a wireless-powered IRS-based MEC system in which MEC server-attached hybrid access point (AP) allows both the IRS and edge users to harvest energy. The work minimizes the energy consumption of the network by the joint optimization of the offloading decisions, active beamforming of the hybrid AP, passive beamforming, and energy harvesting strategies of IRS.

Chu et al. [47] studied the impact of the deployment of an IRS on the computational performance of a MEC system. The work aimed to enhance the performance of the system by intelligent adjustment of the phase shift of IRS elements.

Kumar et al. [48] constructed the video caching challenge as an integer linear programming (ILP) problem for hit-rate optimization. Since the optimization issue necessitates awareness of all upcoming queries, it cannot be employed in real-time. As a result, the work created the RAN-aware Adaptive Video caching (RAVEN) approach. It leveraged network data to generate an intelligent action for video bitrate allocation in video caching paired with transcoding and increased the number of subscribers served from the network edge server.

Xu et al. [49] studied an IRS-assisted NOMA-based MEC system that aimed to minimize the total energy consumption of the network by the joint optimization of the transmission time, transmit powers, offloading-task partitions, and phase shift of IRS.

Yang et al. [50] considered an IRS-aided binary offloading-based MEC system for IoT devices. The work aimed to minimize the overall energy consumption of the user devices

by the joint optimization of the CPU frequencies, binary offloading modes, offloading times, offloading powers, and phase shifts of IRS.

Dai et al. [51] proposed a two-tier computation offloading scheme in heterogeneous networks. The work formulated joint user association and computation offloading problems for multi-task edge computing to minimize energy consumption. However, the work considered a 5G wireless network.

Park et al. [52] proposed a novel scheme for MEC-enabled multi-tier networks in which APs serve the users with edge computing facilities by the MEC servers.

Xu et al. [53] developed an energy-conscious computation offloading method that is intended to minimize energy usage. The work examined all AP routings from the source AP to the target AP selecting the quickest way to offload computational activities. Furthermore, the work used the non-dominated sorting genetic algorithm II (NSGA-II) to achieve multi-objective optimizations to minimize computation or task offloading latency and energy usage.

Measurement Model

Communication Model

The research considers a two-tier network formed by a few micro base stations $\mathcal{B} = \{b_1, b_2, \dots, b_n\}$ operating beneath a macro base station \mathcal{K} and m is the serving micro base station. The user devices are $\mathcal{D} = \{d_1, d_2, \dots, d_n\}$. In the case of an IRS-assisted micro cell, the user devices will be served by the micro base station through an IRS.

Conventional Communication Model

The uplink or upstream received power of a standard micro base station is calculated using the equation below (Eq. 1) [54–56],

$$P_{r \in m(\text{UL})}^{\text{Conv.}} = \frac{P_{t \in d}^{\text{UL}} h \lambda^2}{L^\alpha 16\pi^2}, \quad (1)$$

where $P_{t \in d}^{\text{UL}}$ is the transmit power of the user device. $\lambda = c/f_c$ is the signal wavelength of the propagating signal. c indicates the light-propagation velocity in ms^{-1} . Carrier frequency is termed by f_c whose unit is Hz. h denotes the fading coefficient relative to Rayleigh fading that is following exponential distribution having unit mean. $L = \sqrt{(x^d - x^b)^2 + (y^d - y^b)^2 + (z^d - z^b)^2}$ is the separation distance of the micro base station (of the micro cell) located at (x^b, y^b, z^b) coordinates and the user device situated at (x^d, y^d, z^d) coordinates. α indicates the signal power attenuation exponent.

The uplink SIR can be measured by (Eq. 2),

$$S_{r \in m(\text{UL})}^{\text{Conv.}} = \frac{P_{r \in m(\text{UL})}^{\text{Conv.}}}{\sum P_{r \notin m(\text{UL})}}, \tag{2}$$

where $\sum P_{r \notin m(\text{UL})}$ indicates the total interference received by the user device.

The uplink transmission rate is determined by the following equation (Eq. 3) [57–59],

$$R_{r \in m(\text{UL})}^{\text{Conv.}} = \mathcal{W}_{\text{UL}} \log_2 \left(1 + \frac{P_{r \in m(\text{UL})}^{\text{Conv.}}}{\sum P_{r \notin m(\text{UL})}} \right), \tag{3}$$

where \mathcal{W}_{UL} is the uplink bandwidth.

Therefore, the uplink task offloading latency (or required time) can be obtained by (Eq. 4),

$$L_{r \in m(\text{UL})}^{\text{Conv. (Offl.)}} = \frac{\delta_k}{R_{r \in m(\text{UL})}^{\text{Conv.}}}, \tag{4}$$

where δ_k is the offloading payload size or data size of the task.

IRS-Enabled Communication Model

For an IRS-aided micro base station, the uplink received power can be derived by (Eq. 5) [60],

$$P_{r \in m(\text{UL})}^{\text{IRS}} = \frac{M_T^2 N_R^2 G_{\text{Sctr.}} G_T G_R d_x^L d_y^W A^2 \lambda^2 \cos \theta_i \cos \theta_r}{(l_1 l_2)^2 64 \pi^3} P_{t \in d}^{\text{UL}}, \tag{5}$$

where d_x^L and $d_y^W = \lambda/2$. d_x^L is the length and d_y^W is the width of each scattering element of IRS. The transmitter/receiver gains are G_T and G_R . The scattering gain for each scattering element is $G_{\text{Sctr.}} = \frac{4\pi d_x^L d_y^W}{\lambda^2}$. $l_1 = \sqrt{(x^d - x^i)^2 + (y^d - y^i)^2 + (z^d - z^i)^2}$ indicates the separation distance of the user device at (x^d, y^d, z^d) coordinates and IRS positioned at (x^i, y^i, z^i) coordinates.

$l_2 = \sqrt{(x^i - x^b)^2 + (y^i - y^b)^2 + (z^i - z^b)^2}$ is the separation distance of the IRS and the micro base station at (x^b, y^b, z^b) coordinates. M_T is the number of transmitter and N_R is the receiver elements of the IRS. θ_i is the transmit angle between the user device and IRS and θ_r is the receive angle between the IRS and the micro base station. The IRS (elements') reflection coefficient is A . $P_{t \in d}^{\text{UL}}$ is the uplink transmit power of the user device (towards the IRS).

The uplink SIR in the case of an IRS-empowered micro base station can be obtained by (Eq. 6),

$$S_{r \in m(\text{UL})}^{\text{IRS}} = \frac{P_{r \in m(\text{UL})}^{\text{IRS}}}{\sum P_{r \notin m(\text{UL})}}. \tag{6}$$

The uplink transmission rate is obtained by the equation below (Eq. 7),

$$R_{r \in m(\text{UL})}^{\text{IRS}} = \mathcal{W}_{\text{UL}} \log_2 \left(1 + \frac{P_{r \in m(\text{UL})}^{\text{IRS}}}{\sum P_{r \notin m(\text{UL})}} \right). \tag{7}$$

The uplink latency, in this case, can be derived by the following formula (Eq. 8),

$$L_{r \in m(\text{UL})}^{\text{IRS (Offl.)}} = \frac{\delta_k}{R_{r \in m(\text{UL})}^{\text{IRS}}}. \tag{8}$$

SIR Coverage Probability

The user devices are considered to be inside the coverage range of a corresponding micro base station if the uplink SIR of the user device reaches the threshold or qualifying SIR.

Theorem The SIR probability of coverage [61] is defined by the following (Eq. 9),

$$P_{\text{covrg.}} = 1 - \sum_{d \in m} \lambda_d \int_{R^2} \exp \left[- \left(\frac{S_d^{\text{Thr.}}}{P_{t \in d}} \right)^{\frac{2}{\alpha}} \|q_d\|^2 \sum_{i=1}^n \lambda_i P_{t \in i}^{\frac{2}{\alpha}} \right] \times \exp \left(- \frac{S_d^{\text{Thr.}}}{P_{t \in d}} \|q_d\|^2 \right) dq_d, \tag{9}$$

where λ_d indicates the user devices' density. $S_d^{\text{Thr.}}$ denotes the SIR threshold. $P_{t \in d}$ indicates the uplink transmit power (by the user device). λ_i is the interfering base stations' density. $P_{t \in i}$ is the transmit power corresponding to the interfering base stations. q_d is the separation between the receiver and the transmitter. α indicates the factor for signal attenuation.

Proof Corresponding to the principle of coverage probability (Eq. 10),

$$P_{\text{covrg.}} = 1 - \mathbb{E} \left[\left(\bigcup_{d \in m} \bigcup_{q_d \in \phi_d} \text{SIR} > S_d^{\text{Thr.}} \right) \right] \tag{10}$$

where $\mathbb{E}(\cdot)$ defines the expected value and Eq. 10 is stated utilizing the union bound and may be expressed as (Eq. 11) using the Campbell Mecke Hypothesis [62],

$$P_{\text{covrg.}} = 1 - \sum_{d \in m} \lambda_d \int_{R^2} \mathbb{E} \left[\mathbb{P} \left(\frac{P_{t \in d}}{\|q_d\|^\alpha} > S_d^{\text{Thr.}} \cdot I_{q_d} \right) \right] dq_d \tag{11}$$

where $\mathbb{P}(\cdot)$ denotes the probability and I_{q_d} denotes the interference.

Solve for (Eq. 12),

$$\sum_{d \in m} \lambda_d \int_{R^2} \mathbb{E} \left[\mathbb{P} \left(\frac{P_{t \in d}}{\|q_d\|^\alpha} > S_d^{\text{Thr.}} \cdot I_{q_d} \right) \right] dq_d. \tag{12}$$

Assuming that, the propagation path follows Rayleigh fading, the equation becomes (Eq. 13),

$$\sum_{d \in m} \lambda_d \int_{R^2} \mathcal{L}_{I_{q_d}} \left(\frac{S_d^{\text{Thr.}}}{P_{t \in d}} \right) \exp \left(-\frac{S_d^{\text{Thr.}}}{P_{t \in d} \|q_d\|^{-\alpha}} \right) \quad (13)$$

where $\mathcal{L}_{I_{q_d}}(\cdot)$ denote the interference represented through a Laplace transformed pattern. Considering that, the tiers of the considered network are autonomous or self-sufficient (Eq. 14),

$$\begin{aligned} \mathcal{L}_{I_{q_d}}(s) &= \mathbb{E} \left[\exp \left(-s \frac{P_{t \in d}}{\|q_d\|^\alpha} \right) \right] \\ &= \prod_{d \in m} \mathbb{E} \left[\prod_{q_d \in \phi_d} \exp \left(-s \frac{P_{t \in d}}{\|q_d\|^\alpha} \right) \right]. \end{aligned} \quad (14)$$

Since the propagation paths follow the Rayleigh fading pattern, the expression of Eq. 14 yields (Eq. 15),

$$= \prod_{d \in m} \mathbb{E} \left[\prod_{q_d \in \phi_d} \mathcal{L}_{I_{q_d}} \left(\frac{P_{t \in d}}{\|q_d\|^\alpha} \right) \right]. \quad (15)$$

Using the Poisson point procedure (PPP)-based probability constructing function (Eq. 16),

$$\begin{aligned} &= \prod_{d \in m} \exp \left(-\lambda_d \int_{R^2} \left(1 - \mathcal{L}_{I_{q_d}} \left(\frac{P_{t \in d}}{\|q_d\|^\alpha} \right) \right) d_{q_d} \right) \\ &= \prod_{d \in m} \exp \left(-\lambda_d \int_{R^2} \left(1 - \frac{1}{\left(1 + s \frac{P_{t \in d}}{\|q_d\|^\alpha} \right)} \right) d_{q_d} \right). \end{aligned} \quad (16)$$

Using Euler’s Beta function method and quantifying Polar coordinates derived from Cartesian coordinates (Eq. 17),

$$\mathcal{L}_{I_{q_d}}(s) = \exp \left(-s^{\frac{2}{\alpha}} \sum_{d \in m} \lambda_d \left(\frac{P_{t \in d}}{\|q_d\|^\alpha} \right)^{\frac{2}{\alpha}} \right) \quad (17)$$

From Eqs. (13) and (17) the expression for the coverage probability is written as (Eq. 18),

$$\begin{aligned} \mathcal{P}_{\text{covrg.}} &= 1 - \sum_{d \in m} \lambda_d \int_{R^2} \\ &\quad \times \exp \left(-\left(\frac{S_d^{\text{Thr.}}}{P_{t \in d}} \right)^{\frac{2}{\alpha}} \|q_d\|^2 \sum_{i=1}^n \lambda_i P_{t \in i}^{\frac{2}{\alpha}} \right) \\ &\quad \times \exp \left(-\frac{S_d^{\text{Thr.}}}{P_{t \in d}} \|q_d\|^2 \right) d_{q_d}. \end{aligned} \quad (18)$$

□

Corollary The simplified equation for the coverage probability [62] is expressed as follows (Eq. 19),

$$\mathcal{P}_{\text{covrg.}} = 1 - \exp \left(-\pi S_{r \in m(\text{UL})}^{\frac{2}{\alpha}} \frac{\lambda_d S_d^{\text{Thr.} \frac{-2}{\alpha}}}{\sum_i \lambda_i} \right) \quad (19)$$

where $S_{r \in m(\text{UL})}$ is the obtained SIR in uplink (by Eqs. 2 and 6).

Computation Model

The user devices have to conduct a wide range of computing functions, such as online gaming or multiplayer gaming, face recognition or identification, image analysis or quantification, and so on. $\mathbb{T}_k = \{\delta_k, c_k, t_k^{\text{max}}\}$ where, task $k \in d$ represents the computing or computational activities of user devices. The task data packet size is denoted by δ_k , the needed CPU cycles to accomplish each task are denoted by c_k , and the tolerated latency (max) of each task is denoted by t_k^{max} . The user device can either process a task locally or offload a task for remote processing at the MEC of micro base station depending on the computation capacity, battery or power capacity, and task processing latency requirement [63].

Local Computation

Contemplating F^{Loc} is the maximum capacity of the CPU (in GHz) of a user device. In the local computing paradigm, the computing latency of a task (the time it takes for a user equipment to process a task based on its computing capability) may be calculated. (Eq. 20) [63],

$$t_k^{\text{Loc}} = \frac{\delta_k c_k}{F^{\text{Loc}} - \sum_1^n f_k^{\text{Loc}}}, \quad (20)$$

where $\sum_1^n f_k^{\text{Loc}}$ indicates the occupied CPU capacity of a user device by the previous task/tasks.

The task computation overhead in terms of local processing can be expressed by (Eq. 21),

$$\psi_k^{\text{Loc}} = \phi_k^t t_k^{\text{Loc}} + (1 - \phi_k^e) e_k^{\text{Loc}}, \quad (21)$$

where $\phi_k^e, \phi_k^t \in [0, 1]$ indicate the user device power (battery) capacity and task processing and completion time weighting factor. Apparently, $\phi_k^e + \phi_k^t = 1$. If $\phi_k^t > \phi_k^e$ or $\phi_k^t = 1, \phi_k^e = 0$ then the task for processing \mathbb{T}_k is sensitive to latency. If $\phi_k^e > \phi_k^t$ or $\phi_k^e = 1, \phi_k^t = 0$ then it indicates the lower battery capacity of the user device or a high power-consuming task. e_k^{Loc} battery capacity indicator.

Computation Offloading at the Micro Base Station (Without IRS)

In this case, the task T_k may be divided into two parts; one part represents task offload or transfer time or latency, while the other half represents task computing duration at the Edge node. The study ignored the time needed for receiving or computing outcomes from the MEC to the UE because the derived output is typically significantly less in size than that of the raw data size across most circumstances (e.g., fingerprint recognition). F^{Mic} is the MEC’s maximal processing capability (CPU frequency). $\sum_1^n f_k^{Mic}$ is the occupied computation capacity of the MEC server. As a result, the overall time (or latency) for the accomplishment of the task is calculated by (Eq. 22),

$$\begin{aligned}
 t_k^{Mic(Con\text{v.})} &= L_{r \in m(UL)}^{Conv.(Offl.)} + L_{r \in m(UL)}^{MEC} \\
 &= \frac{\delta_k}{R_{r \in m(UL)}^{Conv.}} + \frac{\delta_k C_k}{F^{Mic} - \sum_1^n f_k^{Mic}} \tag{22}
 \end{aligned}$$

Computation Offloading at the Micro Base Station (IRS-Assisted)

The overall task completion time in the case of IRS-aided transmission is measured by (Eq. 23),

$$t_k^{Mic(IRS)} = \frac{\delta_k}{R_{r \in m(UL)}^{IRS}} + \frac{\delta_k C_k}{F^{Mic} - \sum_1^n f_k^{Mic}} \tag{23}$$

Problem Statement and Solution Approach

Problem Statement The work attempted to offload computing workloads (tasks) from the user device to the micro base station if the adequate battery or power level and/or task execution time are not achievable at the user device. As a result, the work began with the assignment of network resources such as optimal power to achieve optimal SIR coverage probability and bandwidth to enable optimal uplink transmission rate to offload latency-sensitive tasks to

the micro base station. Since the data size of the output (of the computed task) will usually be smaller in size the work exempted an analysis of downlink.

Obtain [Optimal Transmit Power $P_{t \in d}^{UL'}$]

S.t.,

C1: Threshold $\mathcal{P}_{covrg}^{Thr.}$

Obtain [Optimal Bandwidth \mathcal{W}'_{UL}]

S.t.,

C1: Optimal $P'_{r \in m(UL)}$ w.r.t. $P_{t \in d}^{UL'}$

C2: Optimal $S'_{r \in m(UL)}$ w.r.t. $P'_{r \in m(UL)}$

C3: Required $R_{r \in m(UL)}^{Req.}$ w.r.t. $S'_{r \in m(UL)}$

In the instance of a limited battery level or power outage, the user device may be able to transfer its work to the micro base station if the objective task is not highly latency-sensitive (depending on the availability of communication and computation resources these types of tasks may be processed after the processing of latency-sensitive tasks).

S.t.,

C1: $F^{Mic} - \sum_1^n f_k^{Mic} \geq f_k^{Req.}$

C2: Battery level of user device < Required level

In the context of a latency-sensitive task, the target and conditions will be as follows,

S.t.,

C1: $F^{Mic} - \sum_1^n f_k^{Mic} \geq f_k^{Req.}$

C2: Task/computation completion time \leq Latency-constraint

Solution approach The work developed two separate algorithms for optimal power, bandwidth allocation, and computation task offloading based on the research target.

Algorithm 1 is developed for SIR-coverage-aware uplink transmission power and bandwidth allocation (for user devices). First, it will determine the optimal transmit power to achieve the required SIR (according to the required or threshold SIR-coverage probability with respect to the selected SIR threshold). Afterward, in terms of the optimal transmit power, it will allocate the required bandwidth to offload and process a computational task within the required latency. The research in the forthcoming section will test the algorithm in the contexts of the conventional and IRS-assisted transmission model for MEC.

Algorithm 1: Uplink Transmit Power and Bandwidth Allocation

```

1: Input: Define input parameters in terms of the considered network (Conv. or IRS-
  assisted) according to the measurement model.
2: Output: Optimal  $P_{t \in d}^{UL'}$ , Optimal  $\mathcal{W}'_{UL}$ , Optimal  $t'_k$ 
3: Calculate: Interference  $\sum_{r \notin m} P_r$ 
4: Set: Threshold SIR  $S_{r \in m(UL)}^{Thr.}$ 
// Optimal Transmit Power Allocation
5: for base value of  $P_{t \in d}^{UL}$  to max value of  $P_{t \in d}^{UL}$  do
6:   Calculate: Received Power  $P_{r \in m(UL)}$ 
7:   Calculate:  $S_{r \in m(UL)}$ 
8:   Calculate: Coverage Probability  $P_{covrg}$ 
9:   while  $P_{covrg} \leq P_{covrg}^{Thr.}$  do
10:      $P_{t \in d}^{UL'} = P_{t \in d}^{UL}$ 
11:     break
12:   end while
13: end for
14: Calculate: Optimal Received Power  $P'_{r \in m(UL)}$ 
15: Calculate: Optimal SIR  $S'_{r \in m(UL)}$ 
16: Calculate: Required Transmission Rate  $R_{r \in m(UL)}^{Req.} = \delta_k / L_{r \in m(UL)}^{Req.(Offl.)}$ 
17: Calculate: Task Processing Latency at MEC  $L_{r \in m(UL)}^{MEC} = (\delta_k c_k) / (F^{Mic} - \sum_1^n f_k^{Mic})$ 
// Optimal Bandwidth Allocation
18: for base value of  $\mathcal{W}_{UL}$  to max value of  $\mathcal{W}_{UL}$  do
19:   Calculate: Transmission Rate  $R_{r \in m(UL)}$ 
20:   while  $R_{r \in m(UL)} \leq R_{r \in m(UL)}^{Req.}$  do
21:      $\mathcal{W}'_{UL} = \mathcal{W}_{UL}$ 
22:     break
23:   end while
24: end for
25: Calculate: Optimal Transmission Rate  $R'_{r \in m(UL)}$ 
26: Calculate: Optimal Offloading Latency  $L_{r \in m(UL)}^{(Offl.)'}$ 
27: Calculate: Optimal Overall Task Completion  $t'_k = L_{r \in m(UL)}^{(Offl.)'} + L_{r \in m(UL)}^{MEC}$ 
28: plot(Coverage Probability  $P_{covrg}$  with respect to  $P_{t \in d}^{UL'}$ )
29: plot ( $t'_k$  with respect to  $\mathcal{W}'_{UL}$ )

```

Algorithm 2 will assist the network to offload a computational task depending on the power consumption of the user device, latency requirements, and available communication

and computation resources at the micro cell base station. This algorithm is mainly developed considering the context of the practical implementation.

Algorithm 2: Computation task offloading

```

1: Input:  $R_{r \in m(UL)}$ ,  $\delta_k$ ,  $c_k$ ,  $F^{Loc}$ ,  $\sum_1^n f_k^{Loc}$ ,  $F^{Mic}$ ,  $\sum_1^n f_k^{Mic}$ 
2: Output: Computation task offloading
3: Determine: Battery or power level/capacity (of user)
4: Calculate:  $t_k^{Loc}$ 
5: Calculate:  $t_k^{Mic}$ 
//Power computing task (Critical Battery/Power Level at User Device and Processing Time
is not a Concern)
6: if  $\phi_k^e = 1$  and  $\phi_k^t = 0$  then
7:   Request for communication channels to the micro base station
8:   if required radio channels are available then
9:     Request for required computational resources
10:    if required computational resources are accessible then
11:      Initiate offloading
12:    else
13:      Wait for required computational resources in the queue
14:    end if
15:  else
16:    Wait for required radio channels in the queue
17:  end if
18: end if
//Time-constraint task (Battery/Power is Sufficient or not a Concern)
19: else if  $\phi_k^t = 1$  and  $\phi_k^e = 0$  then
20:   if Required task completion time  $> t_k^{Loc}$  then
21:     Compute the task at the User Device
22:   else if Required task completion time  $< t_k^{Loc}$  then
23:     if Required task processing time  $> t_k^{Mic}$  then
24:       Request for required radio channels to the micro base station
25:       if required radio channels are accessible then
26:         Initiate offloading
27:       else
28:         Wait for required radio channels in the queue
29:       end if
30:     else
31:       Wait for required computational resources to complete a task within required
task completion time
32:     end if
33:   end if
34: else
35:   Based on the accessibility of appropriate communication and computing capabilities,
the UE can select whether to process the work locally or to transfer the computational task
to the micro base station
36: end if

```

Numerical Results and Discussions

The section contains numerical results or findings as well as related comments on the outcomes of the MATLAB-based analysis. The simulation parameters and values are listed in Table 1.

In Table 1 the transmit power of the macro base station and micro base station [65–69], path loss exponent [70], tier density [71], cell radius [72], data sizes [73–75], CPU cycles [76] are selected as per the mentioned references.

Figure 1 visualizes the task processing capacity of the typical user devices having 2, 3.5, and 4.5 GHz computing capacity (CPU frequency).

Figure 2 shows the optimal uplink transmit power (of the user device) in the case of a conventional (non-IRS) network in terms of SIR-threshold-aware coverage probability.

Figure 3 represents the result of the attainment of required latency (overall task completion time) for a task in terms of optimal bandwidth.

Table 1 Parameters and Values

Parameters	Values
Macro cell area	1000 square m
Micro cell area	200 square m
Macro BS position	Cell-centered
Micro BS position	In conv. model: (100, 100) coordinates/cell-centered, In IRS-assisted model: (0, 0) coordinates
IRS position	Cell-centered
Transmit power of Macro BS	30 W (both conv. & IRS model); 60 W (only IRS model)
Macro BS height	10 m
Micro BS power	10 W (both conv. & IRS model); 15 W (only IRS model)
Micro BS height	5 m
Carrier	100 GHz
IRS transmitter-receiver elements	256 [60]
IRS transmitter and receiver gain	20 dB [60], 15 dB [64]
IRS transmit-receive angles	45° [60]
IRS placement height	6 m
User device height	1.5 m
IRS reflection coefficient	0.9
Path loss exponent (macro cell)	3.5
Path loss exponent (micro cell)	2.0
Density of user devices	$5000/(\pi \times (100)^2)$ per m^2 ; where 100 m is the cell radius
Density of micro BS	$(5000/(\pi \times (100)^2))/20$ per m^2
Density of macro BS	$(5000/(\pi \times (100)^2))/50$ per m^2
Data sizes	500–1650 Bytes (or 4000–13,200 bits)
CPU cycles per bit	750 cycles
User computation capacity	2, 3.5, 4.5 GHz
MEC computation capacity (at micro base station)	50 GHz (max. 10 GHz per user)

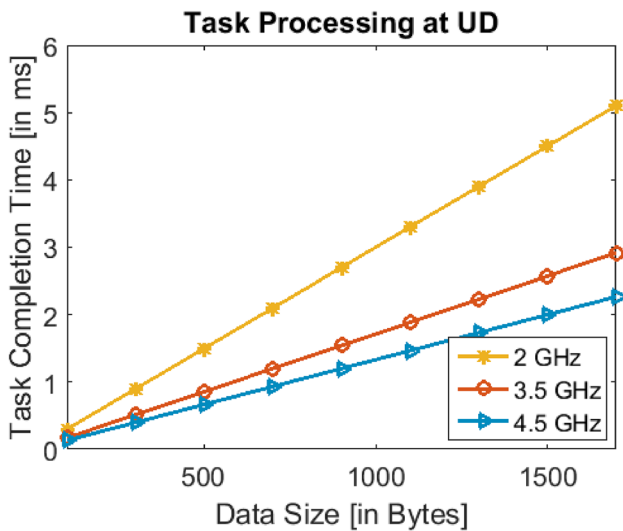


Fig. 1 Task processing capacity of the user devices

Figure 4 visualizes the optimal transmit power in the case of an IRS-assisted multi-tier network in terms of SIR-threshold-aware coverage probability.

Figure 5 shows optimal bandwidth to achieve the required overall task completion time for a task in the context of an IRS-assisted network.

Figure 6 illustrates the variation of transmit power in uplink due to the increase of interference (by the macro and micro base stations) in the case of the IRS-assisted network. Since in the case of the conventional model the research already derived that a significantly higher uplink power is required compared to the IRS-assisted model, therefore, the work intentionally exempted this analysis (with increased interference) for the conventional model.

Figure 7 visualizes a comparative study between this work and prior works in terms of data/task size and task completion time.

Figure 8a, b show the comparative SIR-threshold-aware coverage probability analysis for both the conventional and IRS-assisted model considering a 5 dB of SIR threshold.

By the observation of Fig. 1 it is realizable that, user devices with 2, 3.5, and 4.5 GHz computing capacity can

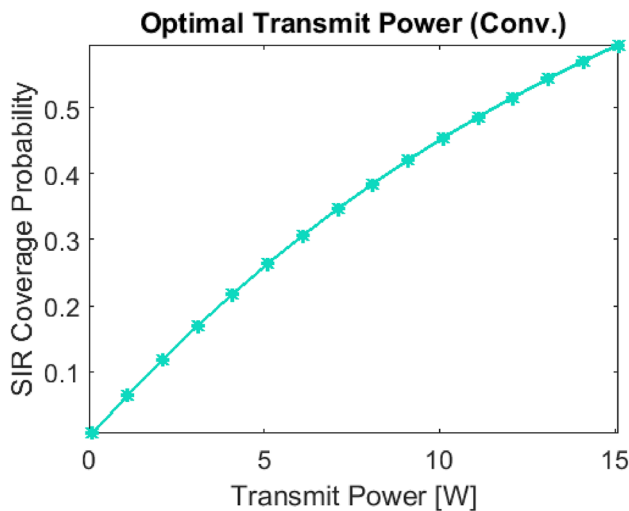


Fig. 2 Optimal transmit power (Conv. model)

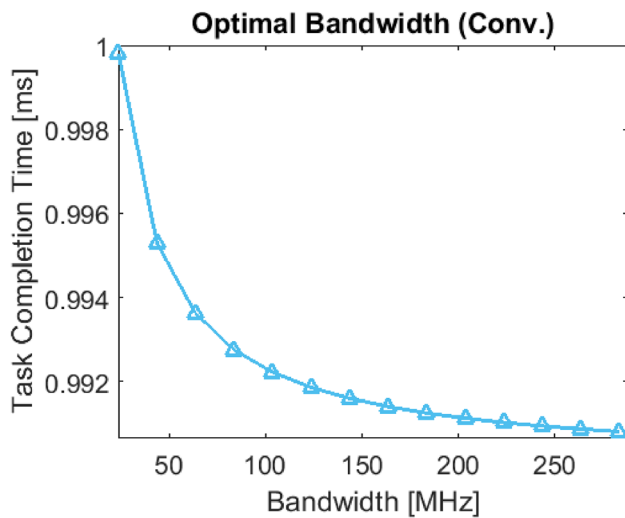


Fig. 3 Optimal bandwidth (Conv. model)

process up to 300, 500, and 700 bytes of data size or payload within less than 1 ms (according to the latency requirement of 6G).

The realization of Figs. 2 and 3 states that in the case of a conventional (non-IRS) multi-tier network approximately 15.2 W of transmit power and up to 288 MHz bandwidth is required to complete a task (offload and process) 1650 bytes of data within less than 1 ms (0.991–1 ms).

From Figs. 4 and 5, it is realizable that, in an IRS-assisted multi-tier network approximately 1.4 W of transmit power and up to 23.2 MHz bandwidth are required to offload and completely process 1650 bytes of data within less than 1 ms (0.991–1 ms).

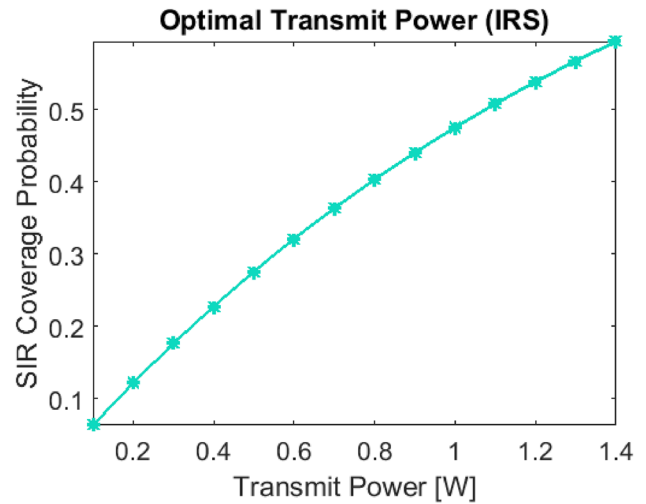


Fig. 4 Optimal transmit power (IRS-assisted model)

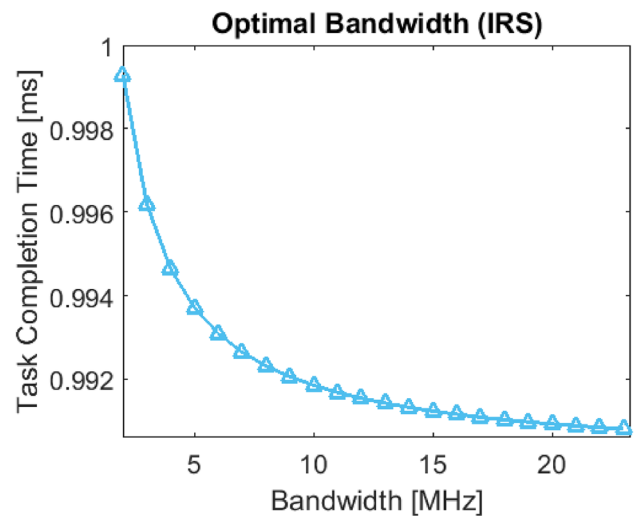


Fig. 5 Optimal bandwidth (IRS-assisted model)

Through the comparison of Figs. 2, 3, 4 and 5 it is comprehensible that, the deployment of IRS can significantly reduce the uplink transmit power and bandwidth. Moreover, the deployment of IRS can be a feasible solution to assure energy and bandwidth efficiency for user devices.

Observing Fig. 6 it is realizable that, due to the increased level of interference a bit extended uplink transmit power (i.e., 2.2 W) is required. Since the required uplink transmit power got increased (Fig. 6) to achieve the threshold SIR-coverage probability the SIR will be the same as the previous one, therefore, there is no variation in the uplink bandwidth. That means the optimal uplink bandwidth remains the same in this circumstance as well.

The comparison of Figs. 4 and 6 states that, when the interference got increased to achieve the threshold SIR

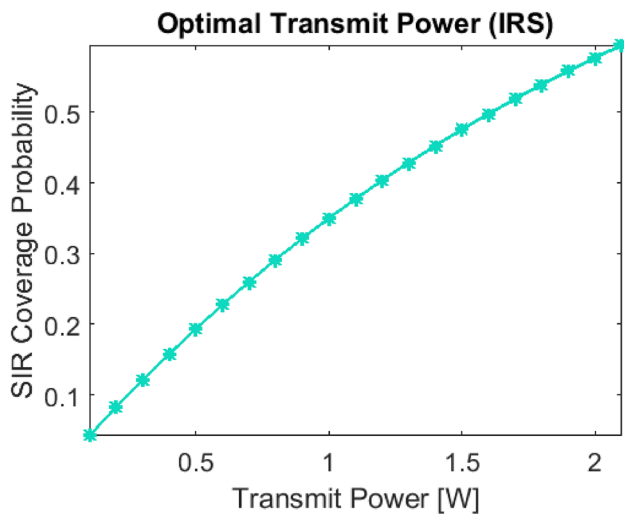


Fig. 6 Optimal transmit power in terms of increased interference (IRS-assisted model)

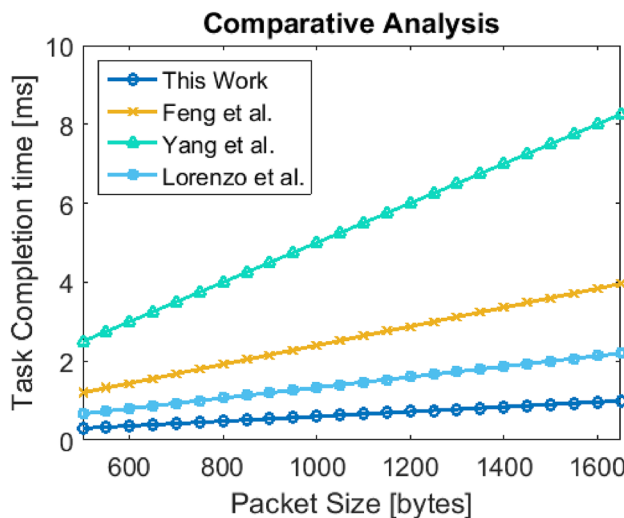


Fig. 7 Comparative analysis

coverage probability a bit increased uplink transmit power is required. However, it is not much significant (only 0.8 W compared to the increased level of interference) and still significantly lower compared to the conventional model. Therefore, it can be stated that the IRS-assisted communication channel can tolerate high interference without significantly increasing the uplink transmit power. Hence, the deployment of the IRS is maintaining energy efficiency.

From Fig. 7 it is realizable that, the developed system can satisfactorily complete all the tasks (of chosen data size) within the threshold task completion time (overall latency) compared to the reference works [77–79].

According to the comparison of Fig. 8a, b, in the case of conventional and IRS-assisted network models the

minimum, i.e., cell edge SIR coverage probability is 0.25 and 0.91, respectively. From Fig. 8a, b it is comprehensible that, with a notably reduced or lower transmit power the deployment of IRS in a micro cell base station provides significantly better coverage over a wide coverage region compared to a conventional non-IRS network.

Table 2 summarizes the derived results.

Research Outcomes The outcomes of the work are enlisted below:

- The developed algorithm for optimal power and bandwidth allocation successfully allocates the power and bandwidth required to complete a computation task within the threshold time/latency.
- The resource allocation algorithm is tested in terms of both conventional and IRS-assisted network models.
- In the case of a conventional network model much higher uplink transmit power is required which may not be feasible for handheld devices such as smartphones since these types of gadgets are power/battery constrained.
- The deployment of IRS reduces the uplink transmit power for user devices, i.e., an 87–91% reduction in uplink transmit power will assure significant energy efficiency for user devices.
- The work derived that the usage of bandwidth gets 92% reduced because of the deployment of IRS in a micro cell.
- If the interference got increased the uplink transmit power required to be increased a bit to obtain optimal task offloading and completion latency but it has no impact on bandwidth because it remains the same (the work considered only the IRS-assisted model for this analysis since the required uplink transmit power in the case of the conventional model is much higher already).
- The implementation of IRS permits a network to set a higher level of SIR threshold compared to the conventional model.
- The deployment of the IRS improves the SIR coverage probability at the cell edge up to 72.5%.

Research Limitations and Future Directions The limitations of this research and future research directions are enlisted below:

- The effectiveness of the algorithms will be fully realized by deploying them in a real-time network.
- The model can be modified and extended for more than two tiers of base stations, e.g., pico and femto cell base station tiers can be considered for future research.
- The model and algorithms can be analyzed considering other enabling or enhancement technologies such as UAV, relay, etc.

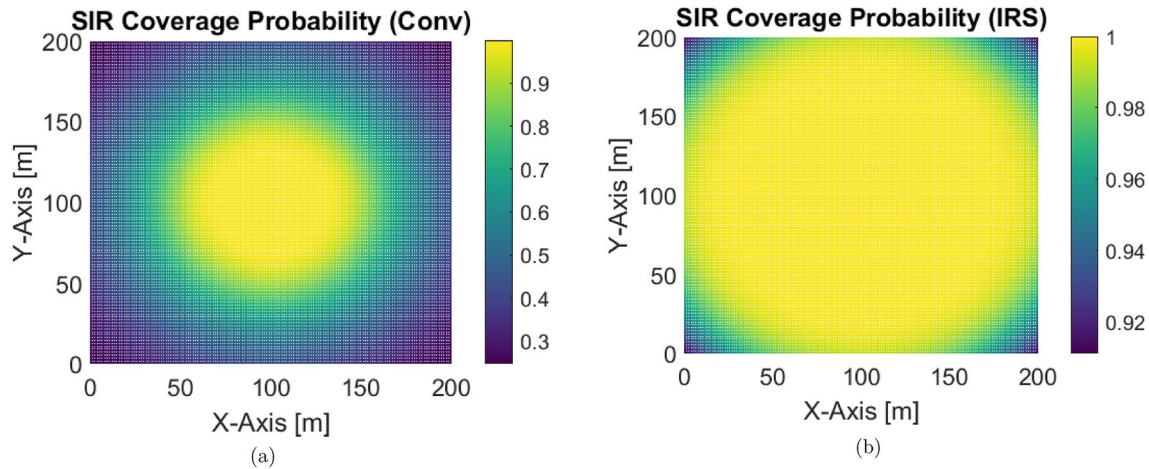


Fig. 8 a SIR coverage probability for a conventional network (15 W), b SIR coverage probability for an IRS-assisted network (1.5 W)

Table 2 Summary of the results

Metrics	Conventional network	IRS-assisted network
Transmit power	15.2 W	1.4 W; 2.2 W (due to the increased level of interference)
Bandwidth	288 MHz	23.2 MHz
Cell edge SIR coverage probability	0.25	0.91

- Sub-THz and THz carriers-based modification of the model and analysis is encouraged for future works.
- Artificial intelligence (AI)/machine learning (ML)-based algorithms such as convolutional neural networks, federated learning, and deep reinforcement learning can be used for resource allocation and task offloading.

Conclusion

The research targeted the enhancement of a MEC-enabled two-tier network by SIR-coverage probability-aware communication and computation resource allocation to offer a successful task completion in a MEC server within the threshold overall latency time-frame or task completion time requirement. In this context, the work developed a measurement model incorporating conventional and IRS-assisted multi-tier communication model, SIR-threshold-based coverage probability analysis model, and computational model to perform simulation-based analysis by MATLAB. The work developed algorithms for optimal resource allocation and task offloading. The developed algorithm successfully derived the optimal transmit power and bandwidth to offload a task to a MEC server to complete the processing of a task

within the threshold. The work compared the communication resource allocation algorithm in the context of both the conventional and IRS-assisted multi-tier communication model. It obtained that the deployment of IRS significantly reduces the uplink transmit power and bandwidth consumption. Moreover, the research found that the implementation of IRS enables the multi-tier network to tolerate a higher level of SIR threshold and interference.

Acknowledgements The authors would like to express gratitude to the Department of Electrical and Computer Engineering, New York University (NYU) Abu Dhabi, Abu Dhabi, UAE.

Funding Not applicable.

Availability of Data and Material Not applicable.

Code Availability Not applicable.

Declarations

Conflict of interest The authors’ declare no known competing interest.

Ethics approval Not applicable.

References

1. Dangi R, Lalwani P, Choudhary G, You I, Pau G. Study and investigation on 5G technology: a systematic review. *Sensors*. 2022;22:26.
2. Fourati H, Maaloul R, Chaari L. A survey of 5G network systems: challenges and machine learning approaches. *Int J Mach Learn Cyber*. 2021;12:385–431.
3. Al-Ogaili F, Shubair RM. Millimeter-wave mobile communications for 5G: challenges and opportunities. In: *Proceedings of the 2016 IEEE international symposium on antennas and propagation (APSURSI)*, Fajardo, 26 June-01 July 2016. p. 1003–1004.
4. Mahdi MN, Ahmad AR, Qassim QS, Natiq H, Subhi MA, Mahmoud M. From 5G to 6G technology: meets energy,

- internet-of-things and machine learning: a survey. *Appl Sci.* 2021;11:8117.
5. Jiang W, Han B, Habibi MA, Schotten HD. The road towards 6G: a comprehensive survey. *IEEE Open J Commun Soc.* 2021;2:334–66.
 6. Alsharif MH, Kelechi AH, Albreem MA, Chaudhry SA, Zia MS, Kim S. Sixth generation (6G) wireless networks: vision, research activities. *Chall Potential Solut Symmetry.* 2020;12:676.
 7. Elmeadawy S, Shubair RM. 6G wireless communications: future technologies and research challenges. In: *Proceedings of the 2019 international conference on electrical and computing technologies and applications (ICECTA), Ras Al Khaimah, 19–21 November 2019.* p. 1–5.
 8. Imoize AL, Adedeji O, Tandiya N, Shetty S. 6G enabled smart infrastructure for sustainable society: opportunities, challenges, and research roadmap. *Sensors.* 2021;21:1709.
 9. Wang Z, Du Y, Wei K, et al. Vision, application scenarios, and key technology trends for 6G mobile communications. *Sci China Inf Sci.* 2022;65: 151301.
 10. Rajoria S, Mishra K. A brief survey on 6G communications. *Wirel Netw.* 2022;28:2901–11.
 11. Elayan H, Amin O, Shihada B, Shubair RM, Alouini M-S. Terahertz band: the last piece of RF spectrum puzzle for communication systems. *IEEE Open J Commun Soc.* 2020;1:1–32.
 12. Vecchio M, Azzoni P, Menychtas A, Maglogiannis I, Felfernig A. A fully open-source approach to intelligent edge computing: AGILE's lesson. *Sensors.* 2021;21:1309.
 13. Anwar A, Seet B-C, Hasan MA, Li XJ. A survey on application of non-orthogonal multiple access to different wireless networks. *Electronics.* 2019;8:1355.
 14. Gong S, et al. Toward smart wireless communications via intelligent reflecting surfaces: a contemporary survey. *IEEE Commun Surv Tutor.* 2020;22:2283–314.
 15. Tapio V, Hemadeh I, Mourad A, et al. Survey on reconfigurable intelligent surfaces below 10 GHz. *J Wirel Commun Netw.* 2021:175.
 16. Rokonzaman M, Mishu MK, Amin N, Nadarajah M, Roy RB, Rahman KS, Buhari AM, Binzaid S, Shakeri M, Pasupuleti J. Self-sustained autonomous wireless sensor network with integrated solar photovoltaic system for internet of smart home-building (IoSHB) applications. *Micromachines.* 2021;12:653.
 17. Wang J, Liu Y, Niu S, Song H. Extensive throughput enhancement for 5G-enabled UAV swarm networking. *IEEE J Miniat Air Space Syst.* 2021;2:199–208.
 18. Lu Y, Zheng X. 6G: a survey on technologies, scenarios, challenges, and the related issues. *J Ind Inf Integr.* 2020:19.
 19. Adhikari M, Hazra A. 6G-enabled ultra-reliable low-latency communications in edge networks. *IEEE Commun Stand Mag.* 2022;6:67–74.
 20. Alsabah M, et al. 6G wireless communications networks: a comprehensive survey. *IEEE Access.* 2021;9:148191–243.
 21. Chowdhury MZ, Shahjalal M, Ahmed S, Jang YM. 6G wireless communication systems: applications, requirements, technologies, challenges, and research directions. *IEEE Open J Commun Soc.* 2020;1:957–75.
 22. Hamdan S, Ayyash M, Almajali S. Edge-computing architectures for internet of things applications: a survey. *Sensors.* 2020;20:6441.
 23. Filali A, Abouaomar A, Cherkaoui S, Kobbane A, Guizani M. Multi-access edge computing: a survey. *IEEE Access.* 2020;8:197017–46.
 24. Jahandar S, Kouhalvandi L, Shayea I, Ergen M, Azmi MH, Mohamad H. Mobility-aware offloading decision for multi-access edge computing in 5G networks. *Sensors.* 2022;22:2692.
 25. Aslanpour MS, Gill SS, Toosi AN. Performance evaluation metrics for cloud, fog and edge computing: a review, taxonomy, benchmarks and standards for future research. *Internet Things.* 2020;12: 100273.
 26. Liang B, Gregory MA, Li S. Multi-access edge computing fundamentals, services, enablers and challenges: a complete survey. *J Netw Comput Appl.* 2022:199.
 27. Mahbub M, Shubair RM. Intelligent reflecting surfaces for multi-access edge computing in 6G wireless networks. In: *Proceedings of the 2022 IEEE international IOT, electronics and mechatronics conference (IEMTRONICS), Toronto, 01–04 June 2022.* p. 1–5.
 28. Ge X, Tu S, Mao G, Wang C-X, Han T. 5G ultra-dense cellular networks. *IEEE Wirel Commun.* 2016;23:72–9.
 29. Shrivastava PS, Malviya UK, Meshram M, et al. Efficiency of ultra-dense multi-tier future cellular networks for 5G: a survey. *Wirel Pers Commun.* 2022;122:3269–91.
 30. Kazi BU, Wainer GA. Next generation wireless cellular networks: ultra-dense multi-tier and multi-cell cooperation perspective. *Wirel Netw.* 2019;25:2041–64.
 31. Bi S, Zhang YJ. Computation rate maximization for wireless powered mobile-edge computing with binary computation offloading. *IEEE Trans Wirel Commun.* 2018;17:4177–90.
 32. Feng C, Han P, Zhang X, Yang B, Liu Y, Guo L. Computation offloading in mobile edge computing networks: a survey. *J Netw Comput Appl.* 2022;202: 103366.
 33. Long W, Chen R, Moretti M, Zhang W, Li J. A promising technology for 6G wireless networks: intelligent reflecting surface. *J Commun Inf Netw.* 2021;6:1–16.
 34. Xing Z, Wang R, Wu J, Liu E. Achievable rate analysis and phase shift optimization on intelligent reflecting surface with hardware impairments. *IEEE Trans Wirel Commun.* 2021;20:5514–30.
 35. Taneja A, Rani S, Alhudaif A, Koundal D, Gündüz ES. An optimized scheme for energy efficient wireless communication via intelligent reflecting surfaces. *Expert Syst Appl.* 2022;190:116106.
 36. Okogbaa FC, Ahmed QZ, Khan FA, Abbas WB, Che F, Zaidi SAR, Alade T. Design and application of intelligent reflecting surface (IRS) for beyond 5G wireless networks: a review. *Sensors.* 2022;22:2436.
 37. Zhu Y, Mao B, Kato N. A dynamic task scheduling strategy for multi-access edge computing in IRS-aided vehicular networks. *IEEE Trans Emerg Top Comput.* 2022;10(4):1761–71.
 38. Khoshkholgh MG, Leung VCM. Coverage analysis of max-SIR cell association in HetNets under Nakagami fading. *IEEE Trans Veh Technol.* 2018;67(3):2420–38.
 39. Zhang X, Yang HH, Sun X, Zhu G, Quek TQS, Zhong Z. SIR coverage analysis in multi-cell downlink systems with spatially correlated queues. *IEEE Access.* 2020;8:99832–45.
 40. Chen G, Wu, Q. Computation rate maximization for IRS-aided wireless powered MEC systems. In: *Proceedings of the 2022 IEEE wireless communications and networking conference (WCNC), Austin, 10–13 April 2022.* p. 417–422.
 41. Wang Q, Zhou F, Hu H, Hu, R.Q. Energy-efficient design for IRS-assisted MEC networks with NOMA. In: *Proceedings of the 2021 13th international conference on wireless communications and signal processing (WCSP), Changsha, 20–22 October 2021.* p. 1–6.
 42. Zhou F, You C, Zhang R. Delay-optimal scheduling for IRS-aided mobile edge computing. *IEEE Wirel Commun Lett.* 2021;10:740–4.
 43. Wang F, Zhang, X. IRS/UAV-based edge-computing/traffic-offloading over RF-powered 6G mobile wireless networks. In: *Proceedings of the 2022 IEEE wireless communications and networking conference (WCNC), Austin, 10–13 April 2022.* p. 1272–1277.

44. Park YM, Hassan SS, Tun YK, Han Z, Hong C.S. Joint resources and phase-shift optimization of MEC-enabled UAV in IRS-assisted 6G THz networks. In: Proceedings of the NOMS 2022-2022 IEEE/IFIP network operations and management symposium, Budapest, 25–29 April 2022. p. 1–7.
45. Bai T, Pan C, Ren H, Deng Y, Elakashlan M, Nallanathan A. Resource allocation for intelligent reflecting surface aided wireless powered mobile edge computing in OFDM systems. *IEEE Trans Wirel Commun.* 2021;20:5389–407.
46. Tan Y, Long Y, Zhao S, Gong S, Hoang DT, Niyato D. Energy minimization for wireless powered data offloading in IRS-assisted MEC for vehicular networks. In: Proceedings of the 2022 international wireless communications and mobile computing (IWCMC), Dubrovnik, 30 May–03 June 2022. p. 731–736.
47. Chu Z, Xiao P, Shojafar M, Mi D, Mao J, Hao W. Intelligent reflecting surface assisted mobile edge computing for internet of things. *IEEE Wirel Commun Lett.* 2021;10:619–23.
48. Kumar S, Doddala SV, Franklin AA, Jin J. RAN-aware adaptive video caching in multi-access edge computing networks. *J Netw Comput Appl.* 2020;168:102737.
49. Xu Z, Liu J, Zou J, Wen Z. Energy-efficient design for IRS-assisted NOMA-based mobile edge computing. *IEEE Commun Lett.* 2022;26:1618–22.
50. Yang Y, Gong Y, Wu Y-C. Intelligent-reflecting-surface-aided mobile edge computing with binary offloading: energy minimization for IoT devices. *IEEE Internet Things J.* 2022;9:12973–83.
51. Dai Y, Xu D, Maharjan S, Zhang Y. Joint computation offloading and user association in multi-task mobile edge computing. *IEEE Trans Veh Technol.* 2018;67:12313–25.
52. Park C, Lee J. Successful edge computing probability analysis in heterogeneous networks. In: Proceedings of the 2018 IEEE international conference on communications (ICC), Kansas City, 20–24 May 2018. p. 1–6.
53. Xu X, et al. An energy-aware computation offloading method for smart edge computing in wireless metropolitan area networks. *J Netw Comput Appl.* 2019;133:75–85.
54. Mir T, Dai L, Yang Y, Shen W, Wang B. Optimal femtocell density for maximizing throughput in 5G heterogeneous networks under outage constraints. In: Proceedings of the 2017 IEEE 86th vehicular technology conference (VTC-Fall), Torontonada, 24–27 September 2017. p. 1–5.
55. Hassan N, Fernando X. Interference mitigation and dynamic user association for load balancing in heterogeneous networks. *IEEE Trans Veh Technol.* 2019;68:7578–92.
56. Mozaffari M, Saad W, Bennis M, Debbah M. Optimal transport theory for cell association in UAV-enabled cellular networks. *IEEE Commun Lett.* 2017;21:2053–6.
57. Mozaffari M, Saad W, Bennis M, Debbah M. Performance optimization for UAV-enabled wireless communications under flight time constraints. In: Proceedings of the GLOBECOM 2017—2017 IEEE global communications conference, Singapore, 04–08 December 2017. p. 1–6.
58. Kim W. Dual connectivity in heterogeneous small cell networks with mmWave backhauls. *Mob Inf Syst.* 2016;2016:1–14.
59. Xiao Z, Liu H, Havyarimana V, Li T, Wang D. Analytical study on multi-tier 5G heterogeneous small cell networks: coverage performance and energy efficiency. *Sensors.* 2016;16:1854.
60. Tang W, et al. Wireless communications with reconfigurable intelligent surface: path loss modeling and experimental measurement. *IEEE Trans Wirel Commun.* 2021;20:421–39.
61. Dhillon HS, Kountouris M, Andrews JG. Downlink MIMO HetNets: modeling, ordering results and performance analysis. *IEEE Trans Wirel Commun.* 2013;12:5208–22.
62. Fadoul MM. Rate and coverage analysis in multi-tier heterogeneous network using stochastic geometry approach. *Ad Hoc Netw.* 2020;98.
63. Yang X, Yu X, Huang H, Zhu H. Energy efficiency based joint computation offloading and resource allocation in multi-access MEC systems. *IEEE Access.* 2019;7:117054–62.
64. Lai F-P, Mi S-Y, Chen Y-S. Design and integration of millimeter-wave 5G and WLAN antennas in perfect full-screen display smartphones. *Electronics.* 2022;11:957.
65. ETSI TS 138 104. Base station (BS) radio transmission and reception. 3GPP TS 38.104. version 15.4.0 Release 15. 2019.
66. Jia X, Fan Q, Xu W, Yang L. Cross-tier dual-connectivity designs of three-tier Hetnets with decoupled uplink/downlink and global coverage performance evaluation. *IEEE Access.* 2019;7:16816–36.
67. Chen S, Peng M, Zhang H, Wang, C. Investigation of service success probability for downlink heterogeneous cellular networks with cell association and user scheduling. In: Proceedings of the 2015 IEEE wireless communications and networking conference (WCNC), New Orleans, 09–12 March 2015. p. 1434–1439.
68. Yang X, Fapojuwo AO. Coverage probability analysis of heterogeneous cellular networks in Rician/Rayleigh fading environments. *IEEE Commun Lett.* 2015;19:1197–200.
69. Fereydooni M, Sabaei M, Dehghan M, Taranez M, Rupp M. A mathematical framework to evaluate flexible outdoor user association in urban two-tier cellular networks. *IEEE Trans Wirel Commun.* 2018;17:1559–73.
70. Mustafa HA, Shakir MZ, Sambo YA, Qaraqa KA, Imran MA, Serpedin E. Spectral efficiency improvements in HetNets by exploiting device-to-device communications. In: Proceedings of the 2014 IEEE Globecom workshops (GC Wkshps), Austin, 08–12 December 2014. p. 857–862.
71. Wu H, Tao X, Li N. Coverage analysis for K-tier heterogeneous networks with multi-cell cooperation. In: Proceedings of the 2015 IEEE Globecom workshops (GC Wkshps), San Diego, 06–10 December 2015. p. 1–5.
72. Gopalam S, Hanly SV, Whiting P. Distributed user association and resource allocation algorithms for three tier HetNets. *IEEE Trans Wirel Commun.* 2020;19:7913–26.
73. Zhou W, Xing L, Xia J, Fan L, Nallanathan A. Dynamic computation offloading for MIMO mobile edge computing systems with energy harvesting. *IEEE Trans Veh Technol.* 2021;70:5172–7.
74. Wang F, Zhang X. Dynamic computation offloading and resource allocation over mobile edge computing networks with energy harvesting capability. In: Proceedings of the 2018 IEEE international conference on communications (ICC), Kansas City, 20–24 May 2018. p. 1–6.
75. Lei L, Xu H, Xiong X, Zheng K, Xiang W. Joint computation offloading and multiuser scheduling using approximate dynamic programming in NB-IoT edge computing system. *IEEE Internet Things J.* 2019;6:5345–62.
76. Guo F, Zhang H, Ji H, Li X, Leung VCM. An efficient computation offloading management scheme in the densely deployed small cell networks with mobile edge computing. *IEEE/ACM Trans Netw.* 2018;26:2651–64.
77. Yang X, Yu X, Rao A. Efficient energy joint computation offloading and resource optimization in multi-access MEC systems. In: Proceedings of the 2019 IEEE 2nd international conference on electronic information and communication technology (ICEICT), Harbin, 20–22 January 2019. p. 151–155.
78. Feng L, Li W, Lin Y, Zhu L, Guo S, Zhen Z. Joint computation offloading and URLLC resource allocation for

collaborative MEC assisted cellular-V2X networks. *IEEE Access*. 2020;8:24914–26.

79. Lorenzo PD, Merluzzi M, Strinati EC. Dynamic mobile edge computing empowered by reconfigurable intelligent surfaces. In: *Proceedings of the 2021 IEEE 22nd international workshop on signal processing advances in wireless communications (SPAWC)*, Lucca, 27–30 September 2021. p. 526–530.

Publisher's Note Springer Nature remains neutral with regard to jurisdictional claims in published maps and institutional affiliations.

Springer Nature or its licensor (e.g. a society or other partner) holds exclusive rights to this article under a publishing agreement with the author(s) or other rightsholder(s); author self-archiving of the accepted manuscript version of this article is solely governed by the terms of such publishing agreement and applicable law.



Mobasshir Mahbub received the MSc Engineering degree in Electrical and Electronic Engineering under the Department of Electrical and Electronic Engineering, Ahsanullah University of Science and Technology, Dhaka, Bangladesh. He graduated (September, 2018) in Electronic and Telecommunication Engineering under the Department of Electronics and Communications Engineering, East West University, Dhaka, Bangladesh with an outstanding academic performance (Merit Scholarship

and Dean's List Award). His fields of interest are IoT, 5G/B5G/6G Wireless Communications, UAV-Aided Communication, Multi-Tier Heterogeneous Network, Multi-Access Edge Computing, NOMA, etc. He is currently working as a Graduate Research Assistant at the Department of Electrical and Computer Engineering, New York University (NYU) Abu Dhabi, UAE on a research project relative to the implementation of IRS technology for 6G. Moreover, He is also working as a Research Assistant at the Department of Electrical and Electronic Engineering, Ahsanullah University of Science and Technology, Dhaka, Bangladesh on a research project relative to the LiFi technology. He collaborated with the Department of Electrical and Computer Engineering, New York University (NYU) Abu Dhabi, UAE; Department of Electrical Engineering, Jouf University, Saudi Arabia; Department of Computer Science and Engineering, Independent University Bangladesh (IUB), Dhaka, Bangladesh; Department of Electrical and Electronic Engineering, University of Liberal Arts Bangladesh (ULAB), Dhaka, Bangladesh. He served as a Project Engineer, in Transport Network Rollout Department under the Technology Division of Robi Axiata Ltd., a renowned telecom operator of Bangladesh. He authored four book chapters (in Springer, IGI Global), seventeen (first author in sixteen papers) research papers published in reputed international journals (in Elsevier, Springer, EAI), and twenty two (first author in twenty papers) conference papers published in reputed international conferences (IEEE Sponsored) including IEEE SECON Workshops. He received 'Best Presenter Award' in 'Mobile Communication' track of IEMTRONICS 2022, Toronto, Canada and 'Best Paper Award' in 'Network Architecture' track of IEEE UEMCON 2021, New York, USA for his research papers. He is a Graduate Student member of IEEE. He is a member of IEEE Computer Society, Bangladesh Chapter. He is serving as a voluntary editor for IEEE Communications Society (ComSoc) since 2019. He is also serving as a member of several technical committees of several IEEE communities and societies. He served

as a member of technical program committee and reviewer for 5th and 6th IEEE FMEC Conference, Paris, France, 2020 and 2021. He served as a keynote speaker in several workshops, seminars, and webinars on Microcontroller Interfacing, Embedded System, IoT, and Robotics (EWU, ULAB, and AUST). He is serving as a reviewer for journals of reputed publishers such as Springer, IEEE, ACM, Hindawi, Wiley, Taylor and Francis, De Gruyter, IOP, Sciendo, Tech Science Press, and Emerald and served as reviewer for several international conferences. He is currently engaged in research on 6G transmission analysis.



Raed M. Shubair (Senior Member, IEEE) received the B.Sc. degree (Hons.) in electrical engineering from Kuwait University, Kuwait, in June 1989, and the Ph.D. degree (Hons.) in electrical engineering from the University of Waterloo, Canada, in February 1993, for which he received the University of Waterloo Distinguished Doctorate Dissertation Award. He is currently a Full Professor of electrical engineering affiliated with New York University (NYU), Abu Dhabi. His current and past academic

and research appointments also include Massachusetts Institute of Technology (MIT), Harvard University, and the University of Waterloo. He was a Full Professor of electrical engineering with Khalifa University (formerly, Etisalat University College), United Arab Emirates, from 1993 to 2017, during which he received several times the Excellence in Teaching Award and Distinguished Service Award. He has over 400 publications in the form of articles in peer-reviewed journals, papers in referred conference proceedings, book chapters, and U.S. patents. His publication span several research areas, including 6G and terahertz communications, modern antennas and applied electromagnetics, signal and array processing, machine learning, the IoT and sensor localization, medical sensing, and nano-biomedicine. He is a fellow of MIT Electromagnetics Academy and a Founding Member of MIT Scholars of the Emirates. He is a standing member of the editorial boards of several international journals and serves regularly for the steering, organizing, and technical committees of IEEE flagship conferences in Antennas, Communications, and Signal Processing, including several editions of IEEE AP-S/URSI, EuCAP, IEEE GlobalSIP, IEEE WCNC, and IEEE ICASSP. He is the General Chair of IEEE WCNC 2024. He is also a Board Member of European School of Antennas and the Regional Director of the IEEE Signal Processing Society in IEEE Region 8 Middle East. He is a Founding Member of five IEEE society chapters in United Arab Emirates, which are the IEEE Communication Society Chapter, the IEEE Signal Processing Society Chapter, the IEEE Antennas and Propagation Society Chapter, the IEEE Microwave Theory and Techniques Society Chapter, and the IEEE Engineering in Medicine and Biology Society Chapter. He was a recipient of several international awards, including the Distinguished Service Award from ACES Society, USA, and MIT Electromagnetics Academy, USA. He organized and chaired numerous technical special sessions and tutorials in IEEE flagship conferences. He delivered more than 60 invited speaker seminars and technical talks in world-class universities and flagship conferences. He has served as the TPC Chair for IEEE MMS2016 and IEEE GlobalSIP 2018 Symposium on 5G satellite networks. He served as the Founding Chair for the IEEE Antennas and Propagation Society Educational Initiatives Program. He is the Founder and the Chair of IEEE at New York University at Abu Dhabi. He is an officer of IEEE ComSoc Emerging Technical Initiative (ETI) on Machine Learning for Communications. He is the Founding Director of the IEEE UAE Distinguished Seminar Series Program for which he

was selected to receive, along with Mohamed AlHajri of MIT, the 2020 IEEE UAE Award of the Year. He served as an Invited Speaker for U.S. National Academies of Sciences, Engineering, and Medicine Frontiers Symposium. He holds several leading roles in the international

professional engineering community. He is also an Editor of IEEE Journal of Electromagnetics, RF and Microwaves in Medicine and Biology, and IEEE Open Journal of Antennas and Propagation.